2017

Tidal stream resource assessment uncertainty due to flow asymmetry and turbine yaw misalignment

M. Piano

S. P. Neill

M. J. Lewis

P. E. Robins

Mohammad Reza Hashemi

See next page for additional authors

Authors

M. Piano, S. P. Neill, M. J. Lewis, P. E. Robins, Mohammad Reza Hashemi, A. G. Davies, S. L. Ward, and M. J. Roberts

Renewable Energy 114 (2017) 1363–1375

Contents lists available at ScienceDirect

Renewable Energy

journal homepage: www.elsevier.com/locate/renene

Tidal stream resource assessment uncertainty due to flow asymmetry and turbine yaw misalignment

M. Piano [a, *], S.P. Neill [b], M.J. Lewis [a, b], P.E. Robins [a], M.R. Hashemi [c], A.G. Davies [a], S.L. Ward [a], M.J. Roberts [a]

[a] Centre for Applied Marine Sciences, Bangor University, Menai Bridge, Anglesey, LL59 5AB, United Kingdom
[b] School of Ocean Sciences, Bangor University, Menai Bridge, Anglesey, LL59 5AB, United Kingdom
[c] Department of Ocean Engineering and Graduate School of Oceanography, University of Rhode Island, Narragansett, RI 02882, USA

ARTICLE INFO

Article history:
Received 3 October 2016
Received in revised form
12 April 2017
Accepted 6 May 2017
Available online 7 May 2017

Keywords:
Marine renewable energy
Tidal stream characterisation
Tidal flow asymmetry
Turbine yaw misalignment
Tidal resource assessment and optimisation
Telemac 2D Irish Sea hydrodynamic modelling and ADCP observations

ABSTRACT

The majority of tidal energy convertors (TECs) currently under development are of a non-yawing horizontal axis design. However, most energetic regions that have been identified as candidate sites for installation of TEC arrays exhibit some degree of directional and magnitude asymmetry between incident flood and ebb flow angles and velocities, particularly in nearshore environments where topographic, bathymetric and seabed frictional effects and interactions are significant. Understanding the contribution of directional and magnitude asymmetry to resource power density along with off axis rotor alignment to flow could influence site selection and help elucidate optimal turbine orientation. Here, 2D oceanographic model simulations and field data were analysed to investigate these effects at potential deployment locations in the Irish Sea; an energetic semi-enclosed shelf sea region. We find that observed sites exhibiting a high degree of asymmetry may be associated with a reduction of over 2% in annual energy yield when deployment design optimisation is ignored. However, at the majority of sites, even in the presence of significant asymmetry, the difference is <0.3%. Although the effects are shown to have less significance than other uncertainties in resource assessment, these impacts could be further investigated and quantified using CFD and 3D modelling.

1. Introduction

Tidal currents offer the potential for generating electricity from a highly predictable renewable resource [1,2]. A key first step in progressing towards commercial realization of tidal stream array sites is robust resource assessment. Initial feasibility and characterisation of high energy sites often focuses on peak velocity and a restricted range of water depths. 'First generation' technologies might operate typically in areas with peak flows in excess of 2.5 m s^{-1} and water depths in the range 25–50 m [3]. However, peak values do not provide an accurate indication of the potential power production due to fine scale temporal and spatial variability in flow [4]. The majority of tidal energy convertors (TECs) under development today focus on converting kinetic energy from the tides using a horizontal axis tidal turbine (HATT) design [5]. Resource assessments typically assume that the turbines will be aligned with the instantaneous tidal flow, yet flow which is symmetrical in nature might not occur on both flood and ebb phases of the tidal cycle. This is due to nearshore physical processes such as bathymetric steering that can result in both magnitude asymmetry and directional misalignment between the plane of mean flood and ebb tidal current direction, as discussed by Lewis et al. [3].

Temporal length scales are important when discussing how devices react as the tidal velocity varies in both magnitude and direction at turbulent time-scales (seconds) [6], but also at larger time-scales (hours) as associated with bathymetric steering or large-scale headland eddy systems [3]. Little information exists on temporal response rates of marine turbine ability to adjust rotor plane axis orientation to flow. At the present time, the authors are unaware of any marine turbine in existence (even with the ability to yaw) that can sufficiently handle changes in flow directionality at short timescales (<hours), however, devices such as the Atlantis AR1500 [7] are being developed with the ability to actively adjust their alignment to flow bi-directionality over a tidal cycle. Bu et al. [8] present experimental results for stepper motor controlled wind

* Corresponding author.
E-mail address: m.piano@bangor.ac.uk (M. Piano).

http://dx.doi.org/10.1016/j.renene.2017.05.023

turbine yawing design that suggest a response time of almost 30s for a 20° yaw misalignment angle. As higher order turbulent timescales are inherently more difficult for marine turbine yawing mechanisms to adapt to than mean tidal flow effects, we neglect these timescales in this study. In contrast, non-yawing devices might include power conversion systems that attempt to desensitize the effects of omni-directional tidal flow asymmetry [9]. At present, such systems remain in early development stages and many first generation designs rely on the selection of sites that exhibit minimal flow misalignment in order to maximize power production.

Misalignment between flood and ebb current directions arises due to a number of factors, yet the effect on resource assessment has not been quantified or compared with other uncertainties. In order to harvest the greatest energy yield at such locations, a yawing mechanism may be required. Quantification of acceptable turbine axial flow misalignment limits may be difficult; however, understanding the relative importance of impacts is key to identifying where more complex and costly yawing devices might be better suited to tidal stream energy extraction than their non-yawing counterparts. Polagye and Thomson [10] used single point ADCP mooring observations and applied a theoretical numerical analysis using MATLAB to assess individual locations within Admiralty Inlet (Puget Sound, USA) and estimated that the potential mean power generated by non-yawing devices might be as much as 5% lower than of the power generated by their passive yawing counterparts at the same site. They point out that the penalty for using non-yawing devices increases as directional variation in the flow increases. However, they do not present a method to spatially assess a much larger region using applied numerical model simulations; therefore, in this study, we apply a similar initial approach and further develop a simple methodology to spatially assess a region using a depth-averaged hydrodynamic numerical model (TELEMAC-2D).

Lewis et al. [3] found that ~6% overestimation of the undisturbed kinetic energy resource exists in energetic tidal regions when flood and ebb flow misalignment effects are ignored; however, this impact on resource estimation reduces to <1% in more rectilinear, offshore locations. Assuming more robust analysis, Galloway et al. [11] suggest that power reductions may only become apparent above 7.5° misalignment, with approximately 20% reduction of power for 22.5° directional misalignment. Frost et al. [12] estimate a 7% reduction in peak turbine power for axial flow misalignment of ±10°, with a 1.5% drop in theoretical power available at the rotor face.

A further consideration in site characterisation is flow magnitude asymmetry, i.e. the difference in peak velocity magnitude between the flood and ebb phases of the tidal cycle. Magnitude asymmetry is caused by frictional effects, often called over-tides (occurring as higher harmonics of the M_2 signal). The asymmetry in the magnitude of tidal currents between the flood and ebb phases is described by the interaction between the M_2 (principal semi-diurnal lunar) and M_4 (quarter diurnal lunar) tidal constituents (e.g. Ref. [13]). Asymmetrical regimes lead to unequal power generation during each phase of the tidal cycle, as well as complex cavitation, structural and cyclic loading issues that will both impact performance and device operational lifespan [14,15]. Since turbine power output is proportional to the cube of the flow velocity, even modest magnitude asymmetry can lead to a significant alteration in the power generated [16,17]. Bruder and Haas [18] examined synthetic velocity signals for varying degrees of M_2/M_4 distortion, and found 8–12% difference in calculated energy capture between extreme asymmetry cases, which is dependent upon device characteristics.

We hypothesize that it may be important to resolve current magnitude and direction asymmetry in conjunction with turbine axial yaw misalignment to flow for estimating power production to meet energy demands on a daily and seasonal basis, as these phenomena often occur concurrently in coastal areas. For instance, it may be that directional misalignment and off-axis variation might prove to be less significant where large magnitude power density asymmetry exists between ebb and flood tidal currents. Although not considered during this study, it is entirely feasible that optimisation algorithms might be developed, which help ascertain the optimal turbine alignment angle to flow conditions in order to maximize potential yield and power take off for TECs.

This study aims to inform site selection and turbine installation design criteria by highlighting how simple spatial assessment can inform the need for optimum orientation of a non-yawing TEC, in order to maximize potential energy yields when selecting a location within energetic regions that exhibit complex magnitude and directional asymmetries (so called 'micro-siting'). We investigate the relative impact of flow direction and magnitude asymmetry along with turbine axial yaw misalignment based on the undisturbed theoretical resource. We then assess the potential increase in relative energy yield when consideration is given to optimising the position of a non-yawing device relative to the direction of flow in the combined case of axial rotor misalignment to flow and tidal asymmetry. Finally, we utilize high resolution coastal modelling simulations and acoustic Doppler current profiler (ADCP) data to compare the cases of installations involving a non-yawing versus yawing analysis approach, at a number of potential tidal stream development sites. Through interpretation of these case studies, we suggest a simple assessment methodology to spatially analyse an area for its sensitivity to yield optimisation based on the asymmetry criteria gleaned from harmonic analysis of the observed and/or simulated tidal signal.

2. Theory

2.1. Flow magnitude asymmetry

The tidal constituent M_2 (having frequency $2\pi f_{M2}$, where $f = 1/T$) and the first harmonic M_4 ($4\pi f_{M4}$) numerically combine to describe tidal asymmetry, which is the product of shallow water effects (e.g. friction) [17,19]. The resultant sea surface elevation, η can be expressed as a superposition of these two constituents, driving pressure gradient forces and subsequent tidal velocities, UV:

$$\eta = \alpha_{M2}\cos\left(\frac{2\pi}{T_{M2}}t - \theta_{M2}\right) + \alpha_{M4}\cos\left(\frac{4\pi}{T_{M4}}t - \theta_{M4}\right)$$

$$UV = u\nu_{M2}\cos\left(\frac{2\pi}{T_{M2}}t - \phi_{M2}\right) + u\nu_{M4}\cos\left(\frac{4\pi}{T_{M4}}t - \phi_{M4}\right) \quad (1)$$

Were subscripted values α and $u\nu$ represent tidal constituent amplitudes, θ and ϕ phase, and T the tidal constituent period, over time, t. The relative non-linear distortion and asymmetry in the resultant signal depends upon both amplitude and phase ratio relationships:

$$\frac{\alpha_{M4}}{\alpha_{M2}} \text{ and } 2\theta_{M2} - \theta_{M4} \text{ or } \frac{u\nu_{M4}}{u\nu_{M2}} \text{ and } 2\phi_{M2} - \phi_{M4} \quad (2)$$

Undistorted semi-diurnal tides have amplitude ratios of zero. Distorted, but symmetrical tides have a relative $2\phi_{M2} - \phi_{M4}$ phase velocity difference, ϕ, of $\pm 90^{\circ}$ and an amplitude ratio greater than zero. When the phasing of M_4 lies within the range -90° to 90° relative to M_2 with an amplitude ratio greater than zero, the distorted tide has a greater flood amplitude and can be described as 'flood dominant'. When the relative phasing lies within the range

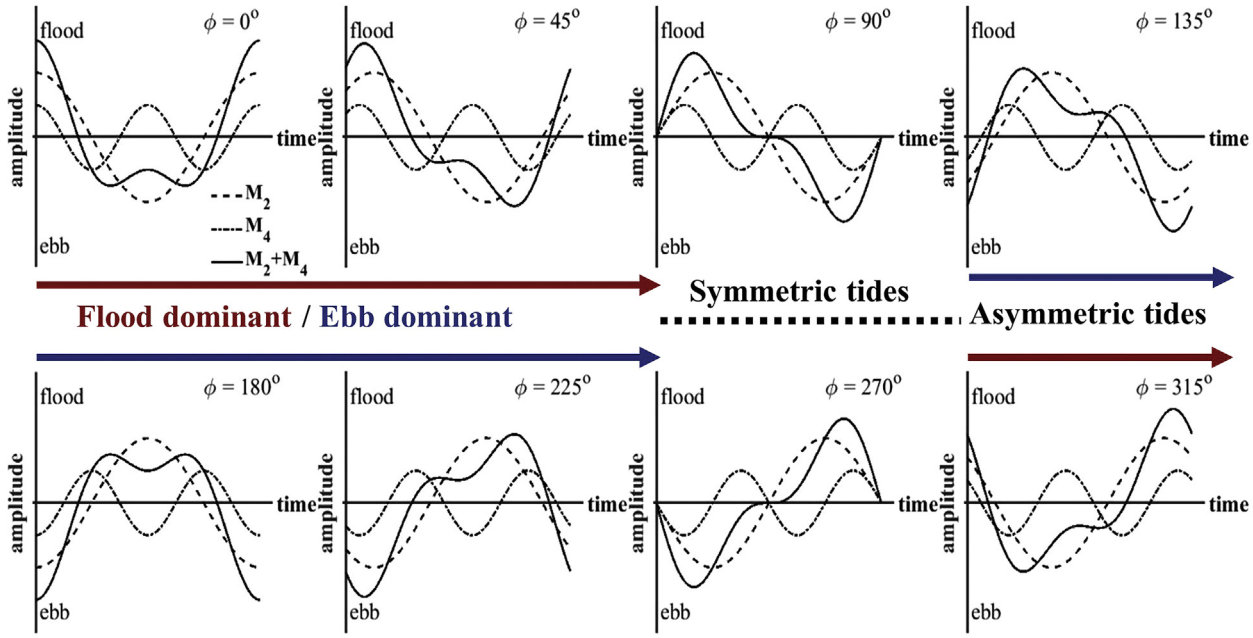

Fig 1. Simulated tidal signal time series when $2\phi_{M2} - \phi_{M4}$ phase velocity difference is flood dominant ($\phi = \pm 90^{\circ}$) and ebb dominant ($\phi = 90 - 270^{\circ}$) producing varying amounts of tidal distortion.

90°–270°, the relationship results in an ebb dominant system (Fig. 1). In either case, the relative distortion of the system will become more pronounced as the amplitude ratio increases [19,20].

Relatively minor distortions in flow magnitude may lead to large changes in theoretical power density, since the available power is proportional to the velocity cubed [12]. A system exhibiting flood or ebb magnitude asymmetry will lead to a corresponding asymmetry in maximum available kinematic power density delivered to the rotor face of a TEC (P_d in W m^{-2}) such that:

$$P_d = \frac{1}{2}\rho\overline{UV}^3 \tag{3}$$

were $\overline{UV}$ is the depth-averaged velocity magnitude (m s^{-1}), and ρ is water density (kg m^{-3}). In the extreme, whereby phase asymmetry of the M_2 and M_4 constituents are 0° and 90° misaligned, this leads to flood dominant asymmetric and distorted symmetric velocity characteristics, respectively (Fig. 2a and b). Here M_4 is assumed to have an amplitude that is 20% of M_2. The maximum exploitable power, P_{max} that can be extracted from the resource can be calculated when specific device characterisation is considered as is outlined in section 3.1. The associated available energy resource, E_{max}, over a complete tidal cycle may then be elucidated (Fig. 2). This analysis shows that the resultant theoretically exploitable energy yield reduces by approximately 30 kWh (~0.6%) for the complete tidal cycle due to the magnitude asymmetry described here alone. What is also clear is that strong asymmetry, arising from complex geomorphology in a region, will lead to a greater potential for power generation over one half of the tidal cycle necessitating careful considerations when micro-siting devices [21].

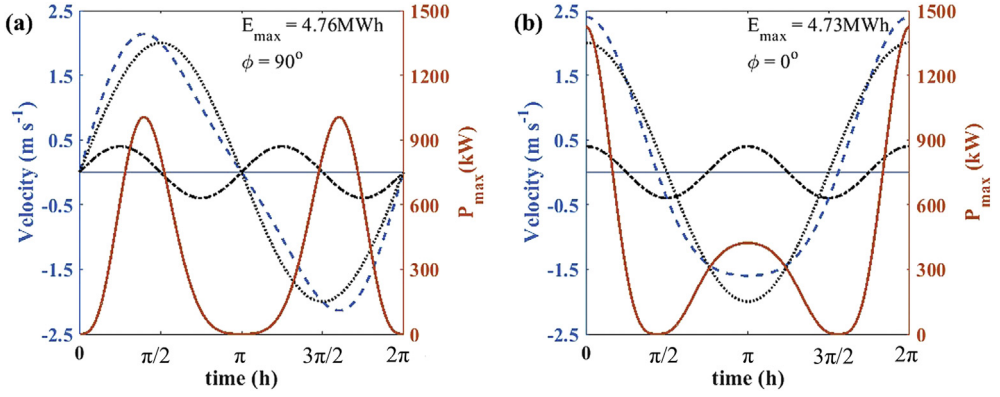

Fig 2. Resultant velocity time series (blue dashed line) produced in the extreme cases when ϕ is (a) 0° and (b) 90° misaligned for the combine M_2 (black dotted line) and M_4 constituents (black dot/dashed line) with M_4 amplitude 20% that of the M_2 amplitude of 2.0 m s^{-1}. The instantaneous maximum theoretical power output (red solid line) and subsequent energy yield, E_{max}, over a tidal cycle is illustrated. (For interpretation of the references to colour in this figure legend, the reader is referred to the web version of this article.)

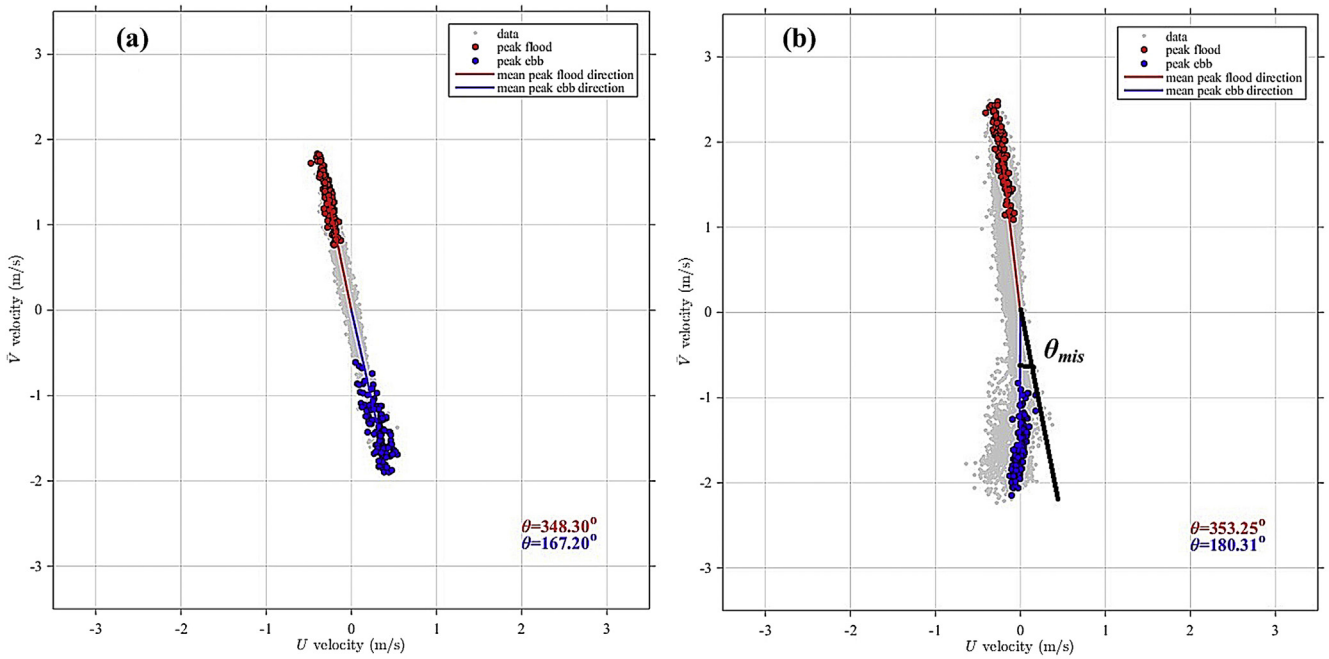

Fig 3. Depth-averaged 10 min ensembles of flow velocity data (grey dots) and subsequent peak flood (red dots) and peak ebb (blue dots) values with associated mean flow direction (red and blue lines) calculated over a complete lunar cycle at two separate moored ADCP stations that exhibit differing amounts of bi-directionality. Station (a) being more rectilinear ($\theta_{mis} = 1.1^{\circ}$) while (b) exhibits greater directional asymmetry ($\theta_{mis} = 7.1^{\circ}$). (For interpretation of the references to colour in this figure legend, the reader is referred to the web version of this article.)

2.2. Flow direction asymmetry

Rectilinear tidal currents, flow alternately in approximately opposite ebb and flood directions, experiencing a peak velocity and then slack water during each half of the tidal cycle. In contrast, omni-directional flows typically exhibit significant directional asymmetry during ebb and flood conditions. The amount of asymmetry between the ebb and flood flow can be summarized by computing the difference in bi-directionality between the mean angle of both directions over a complete lunar cycle [22,23], where the misalignment angle (θ_{mis} in degrees) from rectilinear flow can be calculated from the absolute difference between mean peak flood and ebb directions:

$$\theta_{mis} = \left| \left| \overline{\theta_{flood}(t)} - \overline{\theta_{ebb}(t)} \right| - 180 \right| \tag{4}$$

There will occur some deviation from the principal or incident flow axis within both ebb and flood half cycles (Fig. 3). The most rectilinear currents will exhibit greatest incident flow energy, however an inherent degree of deviation from bi-directionality over a tidal cycle will still exist. Highly energetic sites tend towards bi-directional regimes with such areas found to fall within a 20° deviation from the principal axis [9].

2.3. Turbine axial yaw misalignment

Even turbines that are designed to react to omni-directionality in tides may lack sufficient ability to extract energy efficiently from off-axis currents [22], particularly over shorter timescales. Turbine orientation might affect power yield and can be assessed by simulating a varying flow direction angle (γ) relative to the axial plane of the rotor face (Fig. 4).

As many TEC's under development are currently of a fixed yaw design, we assess the extent to which the orientation of the axial plane of the turbine rotor to current inflow affects the power delivered to a TEC by implementing a simple trigonometric function using a cosine relationship:

$$P_d = \frac{1}{2}\rho \overline{UV}^3 \cos(\gamma) \tag{5}$$

To quantify the relative effect of yaw misalignment on turbine performance, a MATLAB script was written to analyse varying γ from 0° to 20° in increments of 0.1°, to derive P_d. The resultant output for three misalignment scenarios ($\gamma = 0, 10, 20^{\circ}$) is plotted in Fig. 5a. The power density is then normalised to peak flow characteristics, (i.e. when the turbine faces the incoming flow

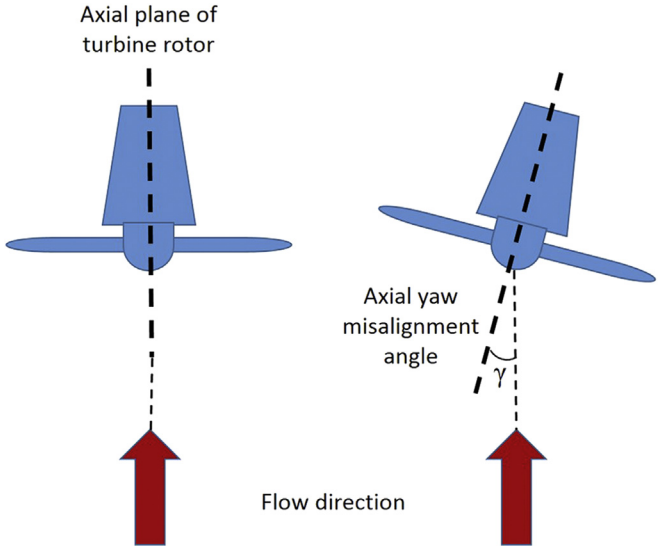

Fig 4. Plan representation of a HATT and the associated axial flow yaw misalignment angle (γ) relative to the turbine rotor axis.

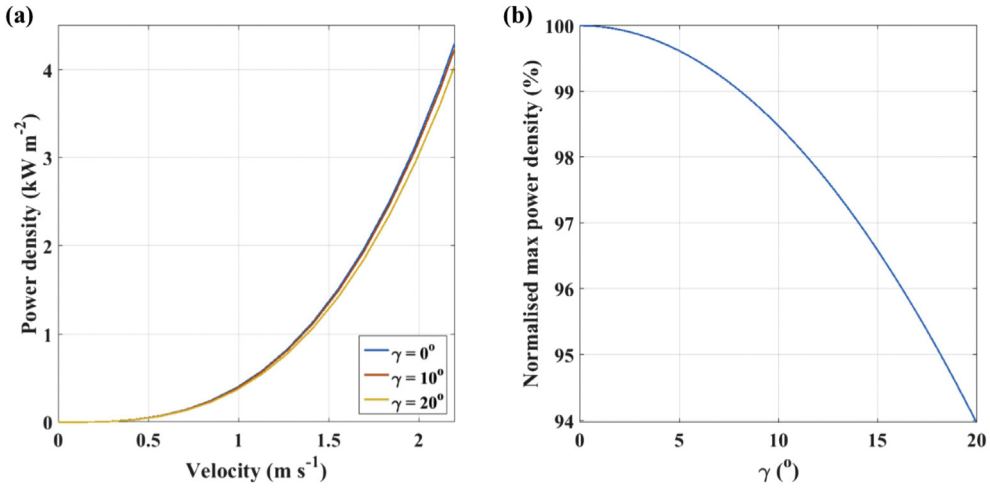

Fig 5. (a) Simulated current velocity versus power density given varying degrees of yaw misalignment angle, γ and (b) resultant normalised maximum power density change for γ values up to 20°.

direction and $\gamma = 0°$) with P_d, found to reduce by up to 6% when $\gamma = 20^{\circ}$ (Fig. 5b); matching Lewis et al. [3].

2.4. Combined effects of asymmetry and misalignment

Typically, tidal asymmetry and yaw misalignment will occur concurrently for applied situations. Therefore, we further consider the combined case of misalignment and asymmetry, maintaining the M_2:M_4 amplitude ratio of 5:1 and varying the phase asymmetry ($2\phi_{M2}$ - ϕ_{M4}) of the tidal velocity signal from $\phi = 0^{\circ}$ to 90° (flood-dominant), in 0.1° increments. Directional asymmetry is also altered for each magnitude asymmetry case from 0° to 20°, in 0.1° increments. In addition, for each scenario described, we vary the cos(γ) relationship in 1° increments. Power density analysed over each tidal cycle is then normalised to the optimum theoretical value (a rectilinear, symmetric tide, i.e. one that exhibits no direction or magnitude asymmetry in the tidal signal). The minimum expected yield (worst case orientation of a TEC) and maximum expected yield (optimal orientation of a TEC) taking into account all possible scenarios of misalignment and asymmetry are plotted in Fig. 6a and b respectively. Exploitable net power density may reduce by up to 5% when optimisation is not considered, while optimal normalised net power density exhibits only 2% maximum difference in the most extreme scenarios.

3. Case study

A variable-resolution TELEMAC-2D hydrodynamic model [24] has been applied to simulate realistic tidal currents in the Irish Sea, a body of water on the western fringe of the British Isles, between the UK mainland and Ireland. It sits at approximately 53° latitude and is fed by tides propagating from the Atlantic Ocean through two restricted inlets, St George's Channel to the south and the North Channel. Strong currents are experienced around the eastern fringe of the sea that includes the Welsh section of the coastline. These currents are created, for the most part, by a semi-diurnal Kelvin wave that propagates within the Irish Sea, generating large tidal ranges along the Welsh coast and strong tidal flows through restricted channels and around headlands and islands such as Anglesey.

[1] The Crown Estate owns the territorial seabed out to 12 nautical miles and manages approximately half (55%) of the foreshore around the UK coastline, some of which is leased to third party management organisations.

The model is centered on northwest Anglesey where the Crown Estate[1] has granted lease rights for a TEC test and development site known as the Morlais Demonstration Zone (MDZ), although the model domain includes other potential tidal development sites such as Ramsey Sound, Bardsey Sound and Amlwch (Fig 7). The recently revised MDZ covers an area of approximately 35 km^2 (Fig. 9a and b). A detailed characterisation of the area highlighted that mean depth-averaged velocities can reach 1.6 m s^{-1} with peak values of 3.7 m s^{-1}. Further, mean neap peak flows of 1.7 m s^{-1} and mean spring peak flows of 3.1 m s^{-1}, were simulated [23]. Although the site is characterized by considerable spatial variation in flow asymmetry and misalignment, this has not been assessed to date (see Section 4).

Model outputs are utilized to assess flow asymmetry and misalignment within the MDZ and to inform the positioning of four ADCP deployments close to the MDZ and for further deployments at the other potential tidal stream sites. MDZ deployments were conducted during research cruises in 2014/2015 to provide *in-situ* velocity measurements for model validation (Fig. 8) and direct resource characterisation (Fig. 9). From the ADCP data, the depth-averaged velocities were determined and then harmonically analysed (Table 2 using MATLAB T_TIDE [25]) to provide variables that allow the estimation of flow magnitude asymmetry (Section 2.1) at each moored MDZ location. Subsequent MATLAB analysis also allows the flow direction asymmetry between the incident flood and ebb angles to be determined (Section 2.2), and further the undisturbed resource potential is assessed when a hypothetical TEC is located at each mooring. Thus we investigate the sensitivity of flow asymmetry and yaw misalignment based on calculating the capacity factor (CF) of a device having generic characteristics (Table 3).

3.1. Turbine parameterisation

A turbine is numerically parameterized in order to assess the significance of variations in the resource at each ADCP location. The power produced, P (and subsequent annual energy yield potential) is calculated as a function of the undisturbed depth-averaged tidal resource velocity using:

$$\begin{aligned} P &= 0 && \left|\overline{UV}\cos^{1/3}(\gamma)\right| < \overline{UV}_c \\ P &= \frac{1}{2}\rho\overline{UV}^3\cos^{\beta}(\gamma)AC_p && \overline{UV}_c \le \left|\overline{UV}\cos^{1/3}(\gamma)\right| \le \overline{UV}_r \\ P &= \frac{1}{2}\rho\overline{UV}_r^3\cos^{\beta}(\gamma)AC_p && \left|\overline{UV}\cos^{1/3}(\gamma)\right| > \overline{UV}_r \end{aligned} \quad (6)$$

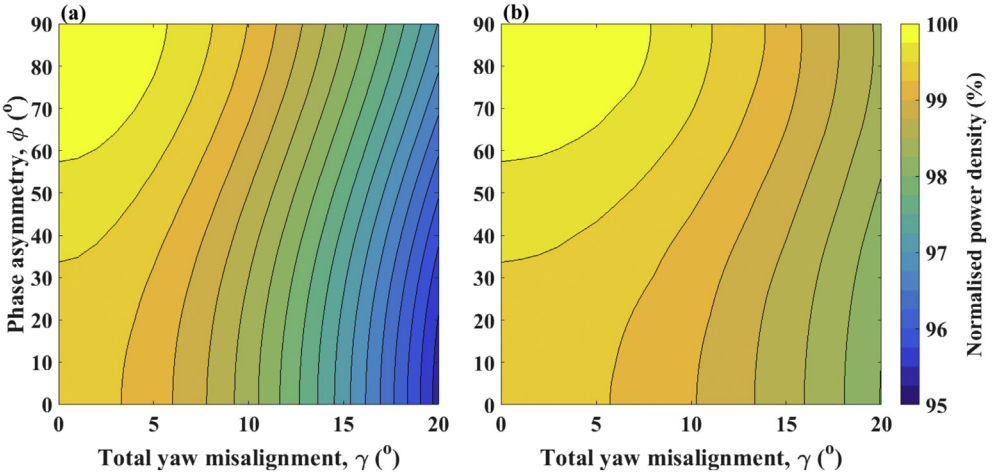

Fig 6. Contour plots of net power delivered to a turbine, normalised by the maximum theoretically extractable value when alignment of the device is (a) non-optimal and (b) optimised for the combined effects of simulated direction and magnitude asymmetry (symmetrical at $\phi = 90^{\circ}$ and distorted flood dominant at $\phi = 0^{\circ}$) and axial flow misalignment using an M_2:M_4 amplitude ratio of 5:1.

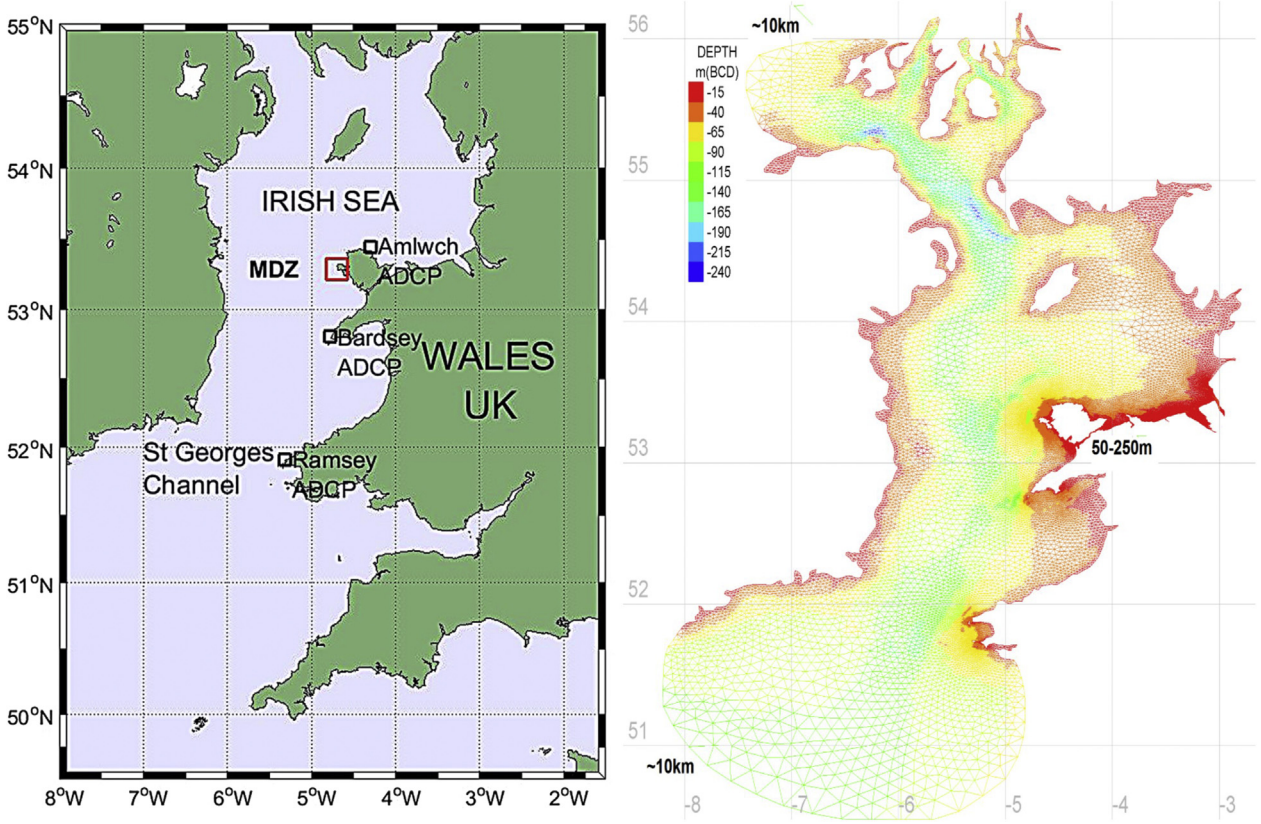

Fig 7. (a) Map of the Irish Sea indicating the location of the Morlais demonstration zone and of ADCP mooring deployments, including one each at Amlwch, Bardsey and Ramsey and a further four in the vicinity of the MDZ (see Fig. 9a, Fig. 9b or Fig. 10b). (b) The discretized TELEMAC-2D model domain, colour scale indicates water depth in metres below chart datum and horizontal grid element resolution is also indicated at boundaries and for the main study area around Anglesey.

A is the turbine rotor swept area (m^2) based on a 16 m diameter, and C_p is the turbine efficiency that increases from 0.38 at cut-in speed ($\overline{UV}_c = 0.5$ m s^{-1}) to 0.45 at rated speed ($\overline{UV}_r = 2.1$ m s^{-1}), these efficiency values are close to those presented by Frost et al. [26]. These characteristics represent a TEC with a water to wire rated output of close to 0.5 MW, which is a more conservative estimate of derived power potential than many previous studies, yet more in line with the present generation of test devices deployed at sea. We utilize simplifying assumptions with regards to losses, e.g. due to turbulent effects, power train efficiency, rotor performance, tip speed ratio etc. by assuming the overall C_p curve as described above incorporates these effects. The yaw misalignment cosine power dependence exponent value, β has been found to vary between 0.5 and 5 in wind turbine assessment reports [27], however, Polagye and Thomson [10] suggest a cosine squared ($\beta = 2$) relationship for marine turbines, although this figure will require further device specific study and analysis in order to robustly quantify.

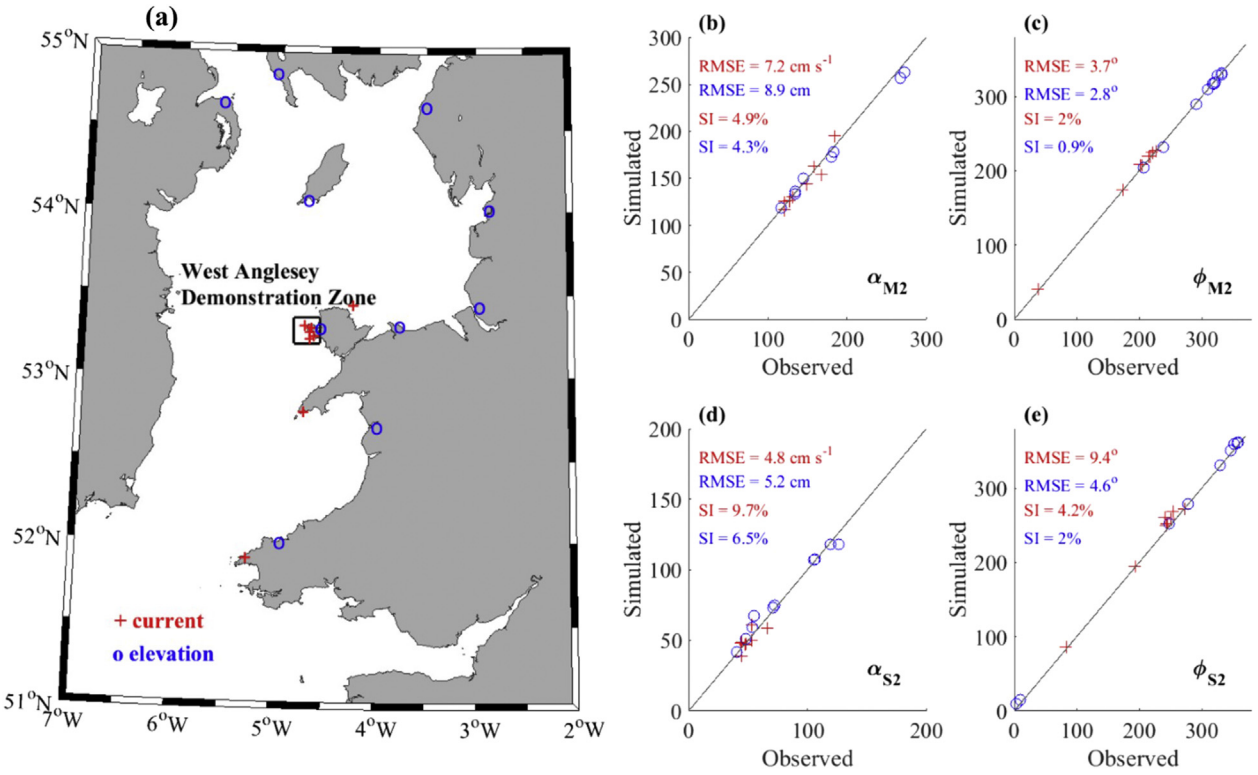

Fig 8. (a) Irish Sea model validation locations. Primary tide gauge stations (blue circles) for surface elevation and seabed mounted ADCP moorings (red crosses) for current amplitudes. Subplots (b) to (e) show regression analysis for M_2 and S_2 amplitude and phase (subscripted α and ϕ respectively) as derived from MATLAB T_TIDE analysis. (For interpretation of the references to colour in this figure legend, the reader is referred to the web version of this article.)

Both yawing and non-yawing devices are considered, with the rotor face assumed to be aligned perpendicular to the incident flood flow angle in the latter instance. For each ADCP time series signal applied, analysis is conducted to determine how altering the orientation of a non-yawing device, in order to ascertain the optimal orientation beyond the initial assumption, might affect yield. For this optimisation, the device orientation is altered in 1° increments between the flood and ebb incident flow angles, assuming undisturbed flow at all times. In each case, the resultant CF is used as a proxy for device performance (Table 3).

3.2. Model setup

TELEMAC-2D (v6.3r2) is an open source, hydrodynamic model, solving the depth-averaged Saint-Venant free surface flow equations derived from the Navier-Stokes equations for momentum and continuity [24]. A finite-element model grid is applied to a domain encompassing the Irish Sea (approximately 50°N to 56°N, 8°W to 3°W). For energetic flow regions in relatively shallow waters, it is assumed that the water column remains vertically mixed, and so the predicted depth-averaged velocities provide a good approximation of flow characteristics.

TELEMAC utilizes an unstructured computational grid, allowing mesh resolution to be refined in regions of interest. Coarse resolution (~10 km) at model boundaries was merged with finer resolution (50–250 m) around the Anglesey coast. The mesh was mapped onto gridded Admiralty Digimap bathymetry data [28] with horizontal resolution of approximately 30 m, corrected to mean sea level (MSL) using the UKHO VORF dataset [29]. TPX07 data containing 13 harmonic constituents (M_2, S_2, N_2, K_2, K_1, O_1, P_1, Q_1, M_4, MS_4, MN_4, M_f and M_m) on a 0.25° resolution structured grid was implemented to provide boundary conditions [30,31,32]. The model boundary forcing comprises surface elevation change and associated horizontal velocities. Additional forcing (e.g., wind, temperature, swell and air pressure) was omitted during simulation, as astronomical tides dominate flows throughout this region [33].

Alternate wetting and drying of intertidal areas was included in the simulation, water density was set to a constant 1025 kg m^{-3}, the Coriolis effect was included and a simple approach was applied to model seabed friction using a fixed coefficient, C, based on Chezy's law that was applied across the entire model domain:

$$C = \frac{R^{1/6}}{n} = \frac{\left(\frac{zh}{2\sqrt{1+z^2}}\right)^{1/6}}{n} \tag{7}$$

Assuming the greatest influence on dynamics is from the largest tidal channel having a broadly triangular shape in the Irish Sea, with hydraulic radius (R) given by the approximate dimensions, 80 km wide (z) and 110 m deep (h), the Manning roughness coefficient (n) for a natural channel was taken as equal to 0.030. The model time step and outputs were set at 10 s and 600 s, respectively. A 35-day simulation and analysis period of a lunar cycle (29.5 days) was adopted, following a model spin-up period of 24 hours.

3.3. Model validation

Simulated outputs of surface elevation and current speed have been compared with depth-averaged *in-situ* measurements for both amplitude and phase of the dominant harmonic M_2 and S_2 constituents at tide gauge and ADCP locations across the Irish Sea. Modelled versus observed root mean square error (RMSE) for amplitude and phase of the dominant constituents along with the associated percentage variance scatter index are presented in Fig. 8b–e. The normalised RMSE indicates simulated M_2 surface elevation amplitude and phase of 4.3% and 0.9%, respectively and

6.5% and 2.0% respectively for S_2. Evaluation of simulated currents gives corresponding values of 4.9%, 2.0%, 9.7% and 4.2%, respectively. The model validation meets the EMEC standard for stage 2b and 3 full-feasibility site assessment [34] and so provides confidence when analysing the undisturbed theoretical resource. The model validation for the M_4 tidal constituent is presented in the Appendix.

3.4. Observations

Teledyne RDI sentinel V_{50} 500 kHz, 5-beam ADCP instruments were fixed in trawl-proof, seabed moorings and deployed in tandem in MDZ locations, concurrently during research cruises in September 2014 and again in March 2015 (Fig. 9). The measurements provided more than 60 days of data from each individual ADCP deployment (Table 1), sufficient to analyse for the main harmonic constituents at all locations (Table 2). The initial deployments (stations #1 and #3) were to the west of the MDZ with measurements made at tidal frequencies (0.067 Hz). Subsequent deployments to the east (stations #2 and #4) were made at 2 Hz. The data was averaged into 10 min (#1, #2 and #4) and hourly (#3) ensembles, having 0.6 m vertical bin resolution. The measurement precision was <0.01 m s^{-1} in all cases. Surface data affected by sidelobe interference from boundary layer interactions was omitted and an interpolated polynomial fit was applied to the vertical profile assuming extrapolated values using a no slip condition at the seabed and constant velocity at the surface before being depth-averaged. Approximate water depths and mean tidal range at the deployment locations were 30–40 m (LAT) and 5.5 m, respectively. Deployments at locations other than north west Anglesey were conducted using Teledyne RDI workhorse 4-beam 600 kHz ADCP's and data was post processed in a similar manner to that described above.

4. Results

The model simulations reveal spatial variability in flow asymmetry and misalignment within the MDZ (Fig. 9a). Both asymmetry and misalignment are stronger nearer to shore, where the depths are shallower and the tidal flow is constrained around headlands

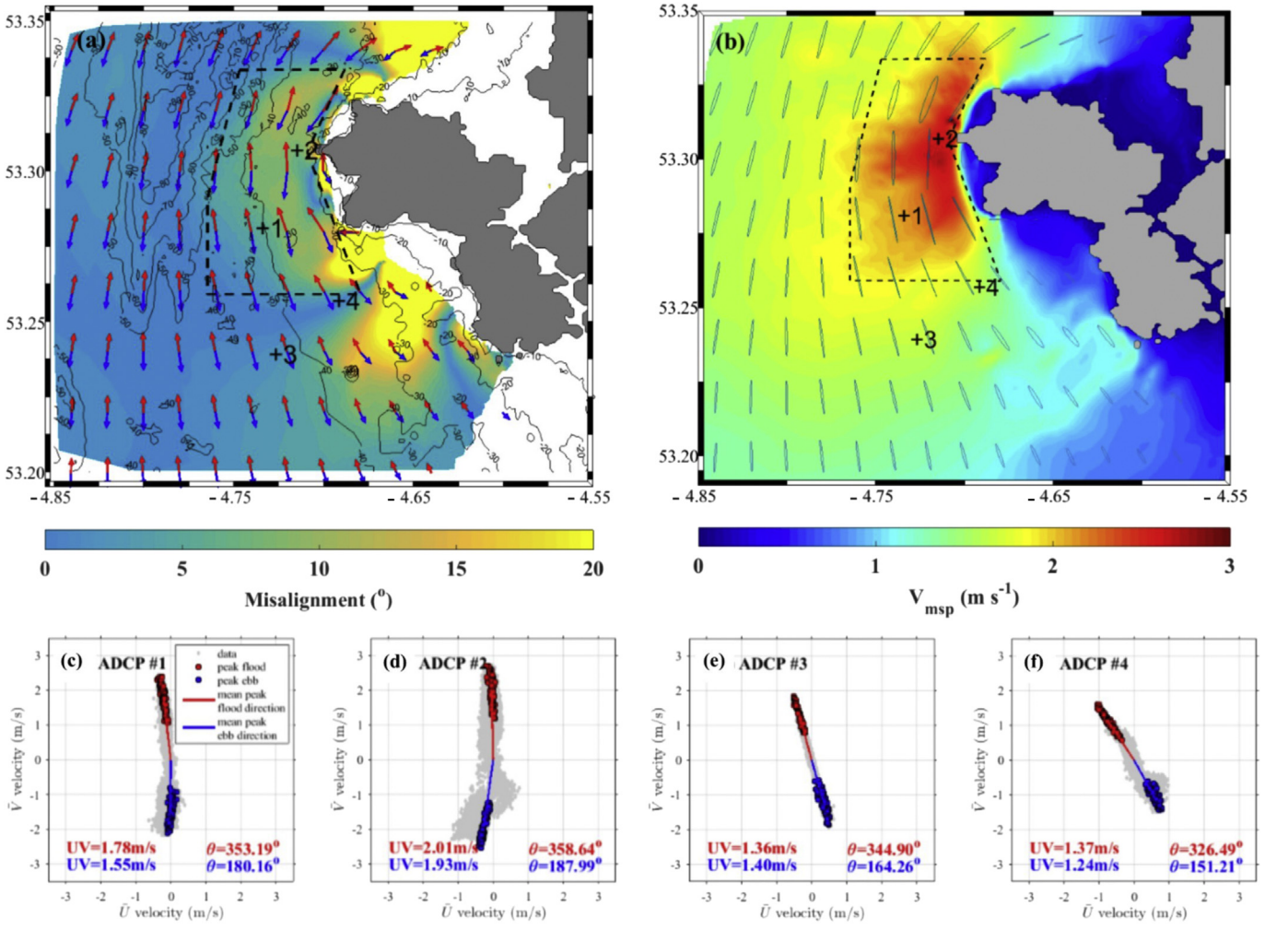

Fig 9. (a) Simulated mean peak flood (red arrows) and ebb (blue arrows) flow magnitude (relative size) and direction. Contour plot illustrates the relative misalignment (θ_{mis}) between mean peak ebb and flood directions (shoreline areas where flow < 0.5 m s^{-1} omitted) with 10 m bathymetric contour lines shown for the region encompassing the MDZ (dashed polygon). (b) Contour plot of mean spring peak velocity, overlaid with M_2 tidal ellipses at discrete points across the region of the MDZ. Subplots (c) to (f) illustrate the depth-averaged $\overline{U}$ and $\overline{V}$ velocity vector scatter plots showing 10 min ensemble data (grey dots) for four ADCP moorings (black crosses in (a) and (b)). Mean peak flood (red) and ebb (blue) magnitude and incident angle of flow are indicated for each station. (For interpretation of the references to colour in this figure legend, the reader is referred to the web version of this article.)

Table 1
ADCP seabed mounted mooring deployments conducted as part of SEACAMS studies.

Position in decimal degrees (WGS 84)		Start date	End date	Deployment Length (days)	Water depth LAT (m)
Latitude	Longitude				
53.28132	−4.73792	19/09/2014	24/11/2014	66.46	43
53.23953	−4.73070	19/09/2014	19/11/2014	61.13	41
53.30708	−4.71853	25/03/2015	27/05/2015	63.13	35
53.25755	−4.69592	25/03/2015	26/05/2015	61.88	36
53.44250	−4.29750	10/02/2014	30/03/2014	47.53	34
52.80280	−4.78320	22/07/2014	22/09/2014	62.25	36
51.91240	−5.31770	01/10/2014	28/11/2014	58.15	34

and islands, and where meso-scale eddy systems form in the adjacent bays. Rectilinear, symmetrical flow is more characteristic of shallow offshore locations where peak tidal velocities are greater (Fig. 9b). Stronger directional asymmetry is exhibited at the ADCP stations closer to shore (#1, #2 and #4), with the more energetic regions to the north of the MDZ exhibiting increased levels compared with the other stations (Table 3). Predominantly flood-dominant asymmetry in the mean peak magnitude values exist according to the simulated results, which is mirrored in the observed analysis (Fig. 9c–f) with greater tendency towards symmetry where rectilinear flow occurs (#4).

The results of the MATLAB T_TIDE harmonic analysis of the tidal current time series for the four ADCP moorings in the MDZ is given in Table 2, with parameters of frequency, amplitude and phase for the three most significant constituents and M_4, presented. Table 3 collates the flow asymmetry and misalignment information along with associated CF calculated for a yawing device, a flood oriented fixed yaw device and an optimised fixed yaw device. CF may be increased by up to 0.1 at the observed locations when consideration to device orientation and optimisation is given. If we consider the CF of a yawing device to be the optimal deliverable yield, then a potential increase in CF from a non-yawing, flood aligned TEC of 0.15%, 0.20%, 0.04% and 0.27% at each of the four sites may be achievable. This shows that when locating a TEC in the locations analysed here tidal asymmetry may be of little significance based on a single device and there is little benefit in considering yawing over fixed yaw devices. However, when these numbers are extrapolated to array scale and disturbed flow and environmental conditions are considered the potential losses in yield may be of increased significance.

5. Discussion

Technical resource assessments for tidal stream development sites require robust spatial and temporal characterisation in order to quantify the potential benefits that the marine renewable energy resource can offer to the electricity generation market. Determining the effect that tidal distortion through asymmetry and turbine misalignment to flow will have on the energy harvested from hydrokinetic power conversion operations may become increasingly important when the sector reaches the commercial array deployment stage. Deployment of monitoring instruments in such highly energetic regions is both difficult, costly and laborious, therefore, robust modelling and simulation techniques offer the potential to quickly assess relatively large domains and areas of seabed being considered for development. Site characterisation for tidal stream arrays should include an assessment of both flow magnitude and direction asymmetry and directional misalignment of the TEC between the ebb and flood incident angles [34], as misalignment of the rotor face to flow effectively alters the power available to the TEC for generation [12].

It has been shown that axial rotor yaw misalignment to incident flow angle (γ) has potentially a greater impact on the theoretical power delivered to the turbine for values > 13° in the symmetrical tide case and > 6° where the tide is asymmetric. The aggregated effect of positioning a non-yawing device in tidal flows exhibiting the characterisics analysed in Section 2.4 could result in up to 5% loss in the exploitable resource power density (Fig. 6a). However, optimisation at the design installation and planning stage could restrict these combined losses to < 2% (Fig. 6b). When the tidal velocity constituent phase difference (ϕ) is < 35° from the symmetrical case and total yaw misalignment to flow direction is < 8°, the orientation of a TEC can be optimised to ensure power density losses remain less than 0.25%. These results correlate well with the estimates of a previous study [3].

When micro-siting a TEC, determination of the importance of design installation and orientation for non-yawing devices would be useful in helping to reduce uncertainty in yield estimates and provide greater confidence for investors. Here, consideration has been given to how to optimise design layout through harmonic analysis and subsequent derivation of tidal constituent parameters, characterised synthetically using simulations and validated directly against observations. We further analyse the simulations and observations to ascertain a proxy for the potential net yield gain, here denoted as the optimisation factor (ξ). The correlation of difference between percentage net gain in annual energy yield ($\Delta AEY = AEY_{opt} - AEY_{nopt}$), or difference between optimised (AEY_{opt}) and non-optimised (AEY_{nopt}) case, versus optimisation factor, which includes a weighted ratio of both tidal asymmetry and misalignment, gives a close relationship to unity, therefore we use this to assess several sites around the Welsh coast (Fig. 10).

$$\xi = \left[(\theta_{mis} * \pi/180) * \left(\frac{\alpha_{M4}/\alpha_{M2}}{|2\phi_{M2} - \phi_{M4}| * \pi/180}\right)\right] * 100 \quad (8)$$

The four MDZ sites, along with data from three further ADCP deployments (see Appendix) conducted at other potential tidal stream development locations in the Irish Sea are included (Fig. 10a). Regression analysis reveals close relationship to 1:1 correlation between ξ and ΔAEY, thus providing a benchmark to predict the potential net gain in energy when assessing the resource at site characterisation stages using hydrodynamic model simulations (Fig. 10b).

This approach highlights whether device orientation may need to be considered and factored into deployment criteria at feasibility study and pre-installation design stages. The magnitude of the potential net gain would be of increased importance at commercial array design and deployment stages. For the MDZ region, the majority of locations within the outlined zone would provide net gains of less than ~0.3% by optimising device orientation to flow and therefore, when compared with similar potential development

Table 2
Main tidal current constituents, together with M_4 analysed for the four ADCP stations in the MDZ.

Tidal constituent	Frequency f (Hz)	Amplitude α (m s^{-1})				Phase ϕ (°)			
		#1	#2	#3	#4	#1	#2	#3	#4
M_2	0.0805	1.579	1.877	1.317	1.215	215.30	204.36	223.55	217.19
S_2	0.0833	0.532	0.593	0.461	0.394	243.83	239.35	252.99	251.31
N_2	0.0789	0.274	0.347	0.228	0.227	174.49	165.16	184.97	175.30
M_4	0.1610	0.122	0.182	0.042	0.047	140.59	132.98	155.40	345.56

Table 3
Assessment of flow asymmetry and misalignment at the four MDZ ADCP stations (decimal degrees, WGS84). Resultant capacity factor is calculated from depth-averaged magnitude and direction velocity time series for a lunar cycle when applied to a TEC having characteristics as described in section 3.1. Three separate device orientation scenarios are presented.

ADCP Station	α_{M4}/α_{M2}	$2\phi_{M2}-\phi_{M4}$ (°)	θ_{mis} (°)	CF		
				yawing	non-yaw flood oriented	non-yaw optimised
MDZ #1 (53.281, −4.738)	0.077	290.01	6.97	33.96	33.77	33.82
MDZ #2 (53.307, −4.719)	0.097	275.74	9.35	50.39	49.90	50.00
MDZ #3 (53.240, −4.731)	0.032	291.70	0.64	22.61	22.59	22.60
MDZ #4 (53.257, −4.695)	0.039	88.82	4.72	18.30	18.16	18.21

sites such as Ramsey and Bardsey (Fig. 10a), the benefits of having to consider device orientation would be of lesser importance. As a further comparison, Hashemi et al. [35] found that wave-current interactions can impact the resource by up to 20% in the extreme, and therefore, the relative significance to such events is low. However for average (e.g. annual) wave-current interaction scenarios, this impact was around 3%, which is comparable with the flow asymmetry and misalignment impacts analysed in this paper. Further, once intra-array wake effects are considered beyond a simplified undisturbed resource study, as conducted here, the impact of device orientation in areas of asymmetric flow may be of greater significance.

Spatial variability of the undisturbed tidal stream resource has been shown to alter dramatically over short distances [23,36]; therefore providing *in-situ* measurements that characterise each potential tidal development location with the purpose of assessing flow asymmetry would be a costly and laborious exercise. A limitation of this study is the assumption of depth-averaged flow in the calculations. However, as the majority of resource assessments use depth-averaged modelling approaches, we sought to quantify some resource estimation uncertainty for flow asymmetry and yaw misalignment using only depth-averaged velocities. A drawback of using 2D models is the inability to account for variations in the vertical structure of velocity in the water column and associated turbulent intensities, which will be important for simulating device feedback, considering that they occupy only a proportion of the entire water column. Future work could investigate the effect when accurately resolving the velocity profile in 3D for resource

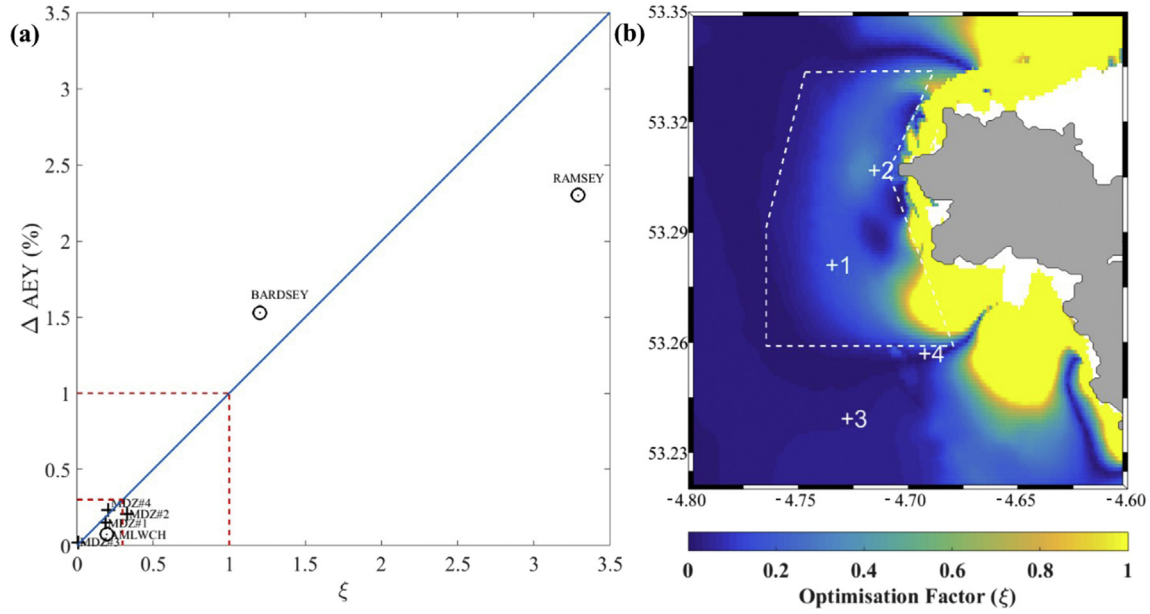

Fig 10. (a) Optimisation factor, ξ, versus difference in annual energy yield for the four MDZ (white dashed polgon) ADCP deployment locations (crosses) plus three other energetic Welsh coastal sites (circles). Reference lines are included for a 1:1 regression fit (blue line) and for values equal to 0.3 and 1 (red dashed lines). (b) An assessment of ξ for the MDZ (shoreline areas where flow <0.5 m s^{-1} omitted). Note that sites at Ramsey Sound and Bardsey Sound exhibit far greater amounts of asymmetry than MDZ and Amlwch locations (see Appendix and Fig. 9) and therefore potential losses through poor design layout and orientation of devices would be greater at those locations than the MDZ locations observed during this study. (For interpretation of the references to colour in this figure legend, the reader is referred to the web version of this article.)

assessments [36,37], by effectively combining environmental feedbacks that enhance flow deceleration with that caused by turbine energy extraction. What may also be important from an asymmetry standpoint is the spread of data from the mean incident flow angle, which is calculated simply as the standard deviation from the mean angle [10].

Increased energy yield might be harvested at commercial array scale as a result of optimising non-yawing devices, simply by considering the orientation of device rotor face to the optimal incident flow direction. The increased cost and complexity of yawing devices in the context of the potential offset from the financial gain in improving potential power yields should also be considered. Accurate modelling assessment focusing on fine scale resource variability could identify the areas that would harness increased amounts of energy through proper device positioning and optimisation, thus allowing high resolution characterisation of entire development zones for commercial scale deployments, therefore reducing investor risk.

6. Conclusion

Both flow asymmetry and axial yaw misalignment have the ability to contribute to a reduction in the technically exploitable power that is available at the point of extraction for a tidal stream turbine. The extent to which the combination of these environmental factors might influence energy extraction has been quantified. For the theoretical tidal velocity time series considered during this study we estimate that optimising turbine orientation to flow dynamics could reduce the potential for losses in annual energy yield to <2% where strong asymmetry occurs and <0.25% where both tidal velocity phase difference is $< 35^{\circ}$ from the ideal symmetrical case and turbine rotor axial yaw misalignment to flow is $< 8^{\circ}$.

When considering the combination of these two factors at sites within the region of the Morlais tidal stream turbine testing and demonstration zone (Anglesey, UK), it has been shown that power density may be affected by <0.3%, based on calculations of capacity factor for a generic turbine using observational data, and by <0.3% for the majority of the zone and other sites around Anglesey when using simulated model spatial assessment based on a parameter we formulate, known as an optimisation factor. Optimising the orientation of a turbine to the incident angle of flow will minimize the potential for losses and improve power yield. For sites at other locations exhibiting a greater optimisation factor, it has been estimated that potential losses in annual energy yield of >2% may arise, where optimal orientation of non-yawing devices is ignored.

Acknowledgements

This work was carried out as part of the Bangor University SEACAMS (Sustainable Expansion of the Applied Coastal and Marine Sectors) and SEACAMS 2 Project (Operation number 80860), part funded by the European Regional Development Fund (ERDF) from the Welsh European Funding Office (WEFO). The study formed part of a collaborative R&D project with Mentor Môn and Morlais, the Third Party Manager for the West Anglesey tidal stream demonstration zone. Tidal model simulations were made possible using Supercomputing (formerly High Performance Computing (HPC)) Wales, a collaboration between Welsh Universities, the Welsh Government and Fujitsu. Data was kindly provided by the British Oceanographic Data Centre (BODC), United Kingdom Hydrographic Office (UKHO) and EDINA Marine Digimap Service. The Authors wish to acknowledge the support of the Sêr Cymru National Research Network for Low Carbon, Energy and the Environment (NRN-LCEE) and the invaluable support of the crew of the RV Prince Madog and technical staff led by Ben Powell at the School of Ocean Sciences, Bangor University. We would also like to acknowledge the input of two anonymous reviewers whose advice helped to improve the overall structure of this manuscript.

Appendix A

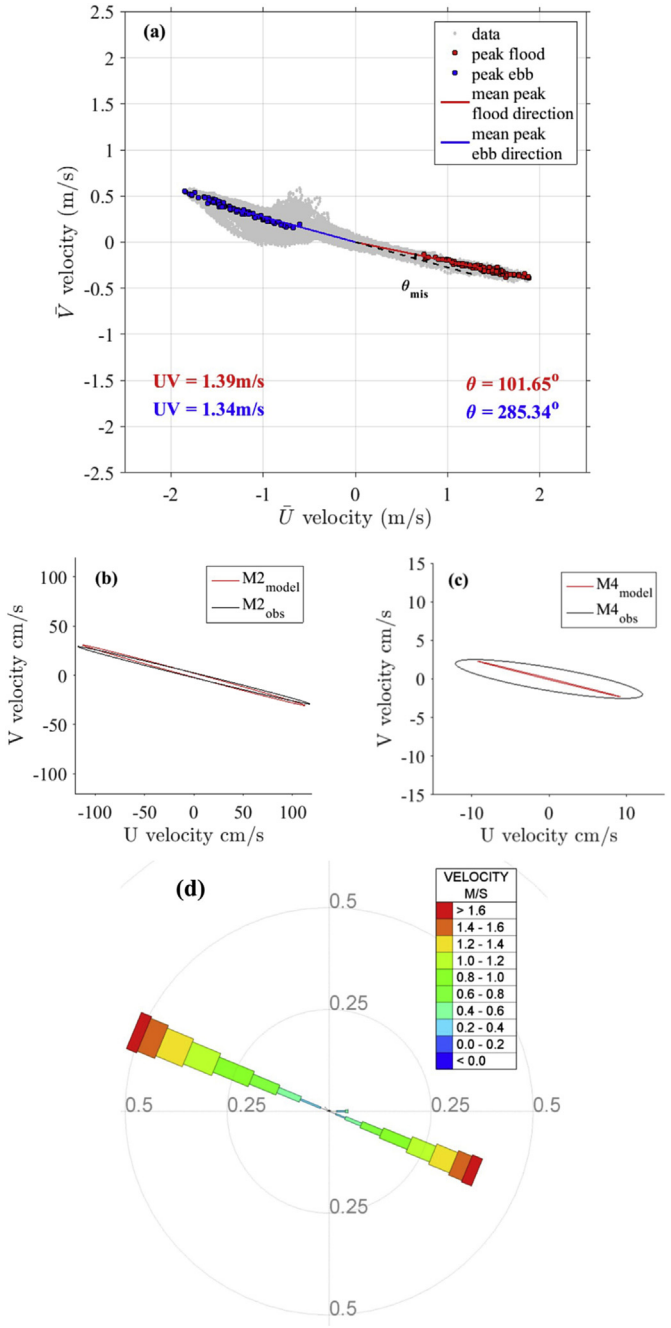

Fig A1. (a) Depth-averaged east and north velocity scatter plot for an ADCP mooring deployed off the Welsh coast near Amlwch (53 26.550°N, 04 17.850°W) with mean peak flood (red) and ebb (blue) values highlighted and incident angle of flow in each direction given. The relative misalignment (θ_{mis}) between mean peak ebb and flood directions can be calculated from Eq (4). Subplots (b) and (c) show the observed and simulated current ellipse for the dominant M_2 and S_2 tidal constituents respectively and (d) is the associated velocity rose output from modelling simulations at the same location.1

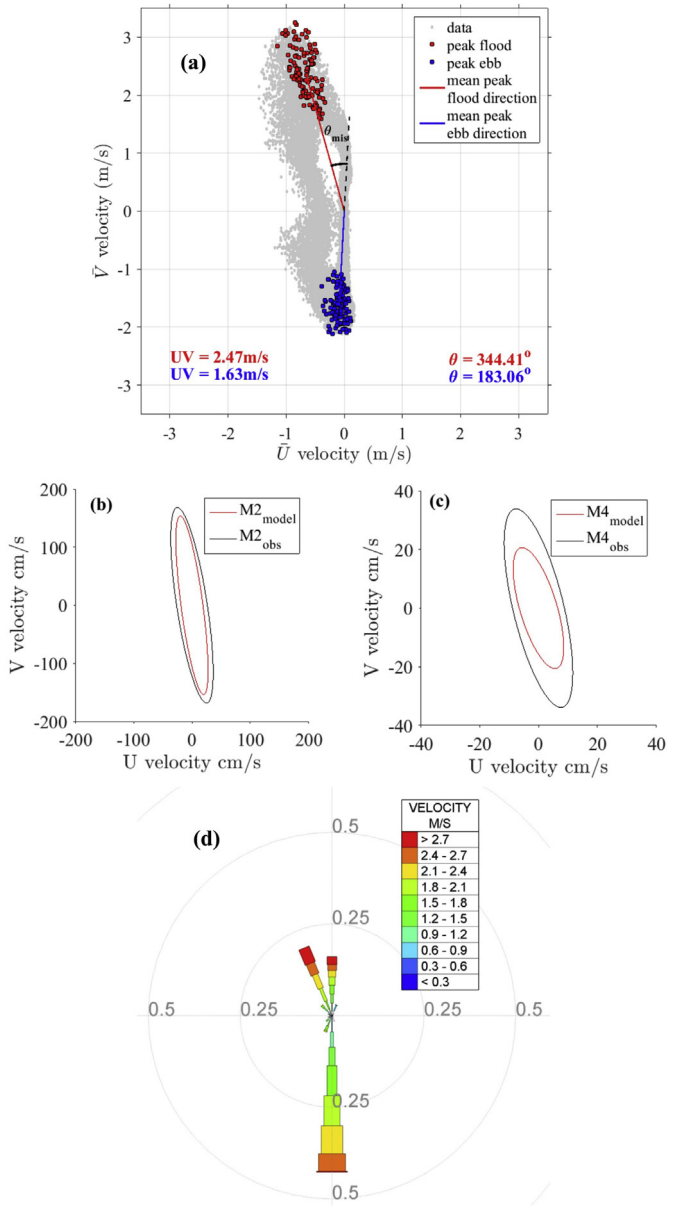

Fig A2. (a) Depth-averaged east and north velocity scatter plot for an ADCP mooring deployed off the Welsh coast near Bardsey Sound (52 48.168°N, 04 46.994°W) with mean peak flood (red) and ebb (blue) values highlighted and incident angle of flow in each direction given. The relative misalignment (θ_{mis}) between mean peak ebb and flood directions can be calculated from Eq (4). Subplots (b) and (c) show the observed and simulated current ellipse for the dominant M_2 and S_2 tidal constituents respectively and (d) is the associated velocity rose output from modelling simulations at the same location.2

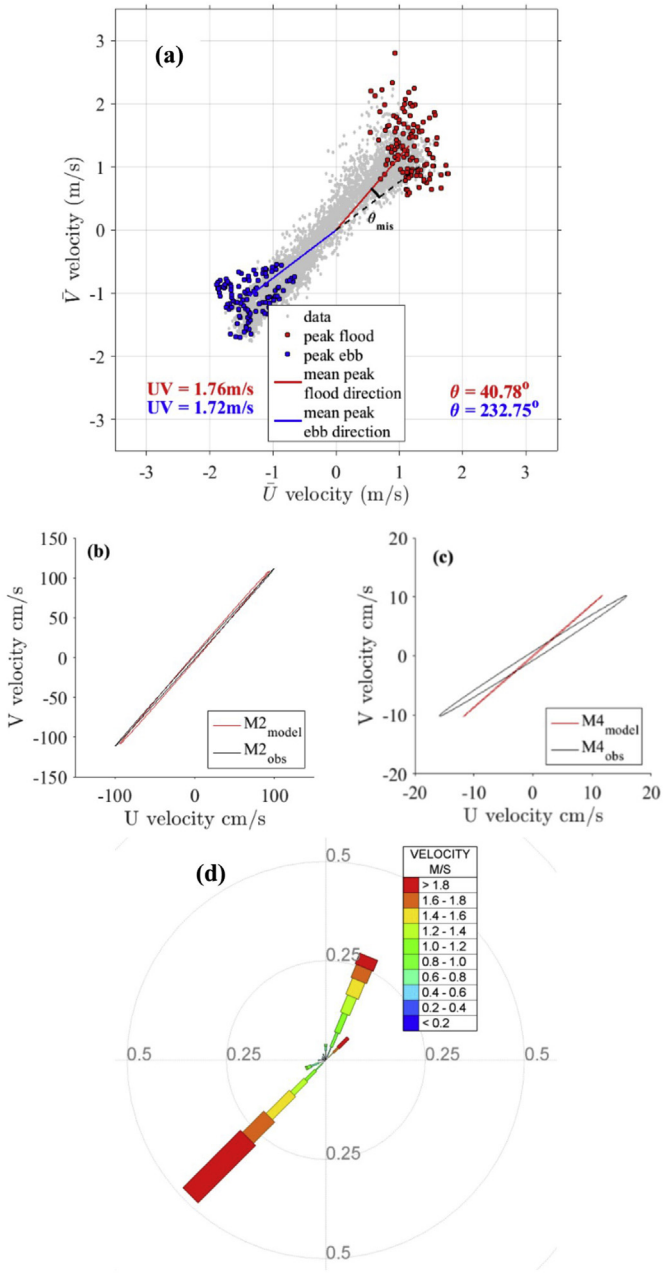

Fig A3. (a) Depth-averaged east and north velocity scatter plot for an ADCP mooring deployed off the Welsh coast near Ramsey Sound (51 54.742°N, 05 19.062°W) with mean peak flood (red) and ebb (blue) values highlighted and incident angle of flow in each direction given. The relative misalignment (θ_{mis}) between mean peak ebb and flood directions can be calculated from Eq (4). Subplots (b) and (c) show the observed and simulated current ellipse for the dominant M_2 and S_2 tidal constituents respectively and (d) is the associated velocity rose output from modelling simulations at the same location.3

Table A1
Assessment of simulated versus observed M_2 and M_4 constituent tidal ellipse parameters at three potential tidal stream development sites in Welsh coastal waters.

Validation Location	M_2 ellipse						M_4 ellipse					
	observed			simulated			observed			simulated		
	major (cm s^{-1})	minor (cm s^{-1})	inc (°)	major (cm s^{-1})	minor (cm s^{-1})	inc (°)	major (cm s^{-1})	minor (cm s^{-1})	inc (°)	major (cm s^{-1})	minor (cm s^{-1})	inc (°)
Amlwch (53.443, −4.298)	121	-2.4	166	117	-2.1	165	12	1.5	170	10	0.1	166
Bardsey (52.803, −4.783)	170	26	99	155	19	98	35	9	104	21	6	107
Ramsey (51.912, −5.318)	150	1.4	48	144	2.5	41	19	0.6	33	16	0.1	41

Appendix B. Supplementary data

Supplementary data related to this article can be found at http://dx.doi.org/10.1016/j.renene.2017.05.023.

References

[1] C. Garrett, P. Cummins, The power potential of tidal currents in channels, Proc. R. Soc. 461 (2005) 2563–2575.
[2] I.G. Bryden, S.J. Couch, ME1-marine energy extraction: tidal resource analysis, Renew. Energy 31 (2006) 133–139.
[3] M. Lewis, S.P. Neill, P.E. Robins, M.R. Hashemi, Resource Assessment for future generations of tidal-sream energy arrays, Energy 83 (2015) 403–415.
[4] P.E. Robins, S.P. Neill, M.J. Lewis, S.L. Ward, Characterising the spatial and temporal variability of the tidal-stream energy resource over the northwest European shelf seas, Appl. Energy 147 (2015) 510–522.
[5] EMEC, "Marine Energy Tidal Stream Developers," [Online]. Available: http://www.emec.org.uk/marine-energy/tidal-developers/. (Accessed 7 September 2016).
[6] J. Thomson, B. Polagye, V. Durgesh, M.C. Richmond, Measurements of turbulence at two tidal energy sites in Puget Sound,WA, IEEE J. Ocean. Eng. 37 (2012) 363–374.
[7] Atlantis Resources Limited, "AR 1500 Brochure," [Online]. Available: https://www.atlantisresourcesltd.com/wp/wp-content/uploads/2016/08/AR1500-Brochure-Final-1.pdf. (Accessed 4 April 2017].
[8] F. Bu, W. Huang, Y. Hu, Y. Xu, K. Shi, Q. Wang, Study and Implementation of A Control algorithm for wind turbine yaw control system, in: 2009 World Non-grid-connected Wind Power and Energy Conference, Nanjing, 2009.
[9] S.F. Harding, I.G. Bryden, Directionality in prospective Northern UK tidal current energy deployment sites, Renew. Energy 44 (2012) 474–477.
[10] B. Polagye, J. Thomson, Tidal energy resource characterization: methodology and field study in Admiralty Inlet, Puget Sound, US, Proc. Inst. Mech. Eng. Part A: J. Power Energy 227 (3) (2013) 352–367.
[11] P.W. Galloway, L.E. Myers, A.S. Bahaj, Experimental and numerical results of rotor power and thrust of a tidal turbine operating at yaw and in waves, in: World Renewable Energy Congress - Marine and Ocean Technology, Linkoping, 2011.
[12] C.H. Frost, P.S. Evans, C.E. Morris, A. Mason-Jones, T. O'Doherty, D.M. O'Doherty, The effect of axial flow misalignment on tidal turbine performance, in: RENEW, Lisbon, 2014.
[13] S.P. Neill, E.J. Litt, S.J. Couch, A.G. Davies, The impact of tidal stream turbines on large-scale sediment dynamics, Renew. Energy 34 (2009) 2803–2812.
[14] R.J. Wood, A.S. Bahaj, S.R. Turnock, L. Wang, M. Evans, Tribological design constraints of marine renewable energy systems, Philos. Trans. R. Soc. Ser. A, Math. Phys. Eng. Sci. 368 (1929) (2010) 4807–4827.
[15] P. Galloway, L. Myers, A. Bahaj, Quantifying wave and yaw effects on a scale tidal stream turbine, Renew. Energy 63 (2014) 297–307.
[16] M.J. Lewis, S.P. Neill, M.R. Hashemi, Realistic wave conditions and their influence on quantifying the tidal stream energy resource, Appl. Energy 136 (2014) 495–508.
[17] S.P. Neill, J.R. Jordan, S.J. Couch, Impact of tidal energy converter (TEC) arrays on the dynamics of headland sand, Renew. Energy 37 (2012) 387–397.
[18] B. Bruder, K. Haas, Tidal distortion as pertains to hydrokinetic turbine selection and resource assessment, in: Proceedings of the 2nd Marine Energy Technology Symposium, Seattle, 2014.
[19] S.P. Neill, M.R. Hashemi, M.J. Lewis, The role of tidal asymmetry in characterizing the tidal energy resource of Orkney, Renew. Energy 68 (2014) 337–350.
[20] C.T. Friedrichs, D.G. Aubrey, Non-linear tidal distortion in shallow well-mixed estuaries: a synthesis, Estuar. Coast. Shelf Sci. 27 (1988) 521–545.
[21] S. Gooch, J. Thomson, B. Polagye, D. Meggitt, Site Characterization for Tidal Power, in: Oceans 2009, MTS/IEEE Biloxi-Marine Technology for Our Future: Global and Local Challenges, 2009, pp. 1–10.
[22] R. Bedard, Survey and Characterization: Tidal in Stream Energy Conversion (TISEC) Devices, in: EPRI North American Tidal in Stream Energy Conversion Feasibility Demonstration Project, 2005.
[23] M. Piano, S. Ward, P. Robins, S. Neill, M. Lewis, A.G. Davies, B. Powell, A. Wyn-Owen, M.R. Hashemi, Characterizing the tidal energy resource of the West Anglesey Demonstration Zone (UK), using Telemac-2D and field observations, in: XXII Telemac & Mascaret Users Conference, Daresbury, 2015.
[24] J.M. Hervouet, Hydrodynamics of Free Surface Flows, John Wiley and Sons, 2007.
[25] R. Pawlowicz, B. Beardsley, S. Lentz, Classical tidal harmonic analysis including error estimates in MATLAB using T_TIDE, Comput. Geosci. 28 (2002) 929–937.
[26] C. Frost, C.E. Morris, A. Mason-Jones, D.M. O'Doherty, T. O'Doherty, The effect of tidal flow directionality on tidal turbine performance characteristics, Renew. Energy 78 (2015) 609–620.
[27] K. Boorsma, Power and Loads for Wind Turbines in Yawed Conditions, ECN, Petten, 2012.
[28] EDINA, "Marine Digimap Service," [Online]. Available: http://digimap.edina.ac.uk. (Accessed 8 May 2015).
[29] United Kingdom Hydrographic Office, VORF Model VORF-UK08, UKHO, 2008.
[30] C.-T. Pham, Use of tidal harmonic constants databases to force open boundary conditions in TELEMAC, in: XIXth TELEMAC-MASCARET User Conference, Oxford, 2012.
[31] G.D. Egbert, A.F. Bennett, M.G. Foreman, TOPEX/POSEIDON tides estimated using a global inverse model, J. Geophys. Res. 99 (C12) (1994) 24821–24852.
[32] G.D. Egbert, S.Y. Erofeeva, Efficient inverse modeling of barotropic ocean tides, J. Atmos. Ocean. Technol. 19 (2002) 183–204.
[33] M.J. Howarth, Hydrography of the Irish Sea SEA6 Technical Report, POL Internal Document 174, Liverpool, 2005.
[34] C. Legrand, Assessment of Tidal Energy Resource, in: Marine Renewable Energy Guides EMEC, 2009. London.
[35] M.R. Hashemi, S.P. Neill, P.E. Robins, A.G. Davies, M.J. Lewis, Effect of waves on the tidal energy resource at a planned tidal stream array, Renew. Energy 75 (2015) 626–639.
[36] M. Thiebaut, A. Sentchev, Asymmetry of tidal currents off the W. Brittany coast and assessment of tidal energy resource around the Ushant Island, Renew. Energy 105 (2017) 735–747.
[37] M. Lewis, S. Neill, P. Robins, S. Ward, M. Piano, M.R. Hashemi, Observations of flow characteristics at potential tidal-stream energy sites, in: EWTEC, Nantes, 2015.